

1  
2  
3  
4  
5  
**Title: Ribosome rescue inhibitors clear *Neisseria*  
6           *gonorrhoeae* *in vivo* using a new mechanism**  
7  
8  
9  
10

11           **Authors:** Zachary D. Aron<sup>1,†</sup>, Atousa Mehrani<sup>2,†</sup>, Eric D. Hoffer<sup>3,†</sup>, Kristie L. Connolly<sup>4</sup>,  
12           Matthew C. Torhan<sup>1</sup>, John N. Alumasa<sup>5</sup>, Pooja Srinivas<sup>3</sup>, Mynthia Cabrera<sup>5</sup>, Divya  
13           Hosangadi<sup>5</sup>, Jay S. Barbor<sup>1</sup>, Steven C. Cardinale<sup>1</sup>, Steven M. Kwasny<sup>1</sup>, Lucas R.  
14           Morin<sup>1</sup>, Michelle M. Butler<sup>1</sup>, Timothy J. Opperman<sup>1</sup>, Terry L. Bowlin<sup>1</sup>, Ann Jerse<sup>4</sup>, Scott  
15           M. Stagg<sup>2,6</sup>, Christine M. Dunham<sup>3</sup>, Kenneth C. Keiler<sup>5,\*</sup>  
16

17           **Affiliations:**

18           <sup>1</sup>Microbiotix, Inc. One Innovation Dr., Worcester, MA 01605, USA

19           <sup>2</sup>Department of Chemistry and Biochemistry, Florida State University

20           <sup>3</sup>Department of Biochemistry, Emory University School of Medicine and Emory Antibiotic  
21           Resistance Center

22           <sup>4</sup>Department of Microbiology and Immunology, Uniformed Services University,  
23           Bethesda, MD

24           <sup>5</sup>Department of Biochemistry & Molecular Biology, Penn State University

25           <sup>6</sup>Institute of Molecular Biophysics, Florida State University

26           \*Correspondence to: [kkeiler@psu.edu](mailto:kkeiler@psu.edu)

27           †These authors contributed equally

28  
29           PDB accession code: 6OM6; EM accession code: EMD-20121

30  
31           Keywords: ribosome, trans-translation, tmRNA, gonorrhea, antibiotic

32  
33  
34           Disclaimer: The contents of this article are solely the responsibility of the authors and do  
35           not necessarily represent the official views of the Department of Defense or the  
36           Uniformed Services University

37

38

39

40

41 **Abstract:** The *trans*-translation pathway for rescuing stalled ribosomes is conserved and  
42 essential in bacterial pathogens but has no mammalian homolog, making it an ideal target  
43 for new antibiotics. We previously reported the discovery of a family of  
44 acylaminooxadiazoles that selectively inhibit *trans*-translation, resulting in broad-  
45 spectrum antibiotic activity. Optimization of the pharmacokinetic and antibiotic properties  
46 of the acylaminooxadiazoles produced MBX-4132, which cleared multiple-drug resistant  
47 *Neisseria gonorrhoeae* infection in mice after a single oral dose. Cryo-EM studies of non-  
48 stop ribosomes showed that acylaminooxadiazoles bind to a unique site near the peptidyl-  
49 transfer center and significantly alter the conformation of ribosomal protein L27,  
50 suggesting a novel mechanism for specific inhibition of *trans*-translation by these  
51 molecules.

52

53 **One Sentence Summary:** Ribosome rescue inhibitors reveal a new conformation of the  
54 ribosome and kill drug-resistant *Neisseria gonorrhoeae* *in vivo*.

55

56

57 **Main text:**

58

59

Antibiotic-resistant bacterial pathogens pose a substantial threat to human health  
60 and are projected to cause up to 10 million deaths per year by 2050 if new antibiotics are  
61 not developed (1). Among the 5 most dangerous “Urgent Threats” identified by the CDC  
62 is drug-resistant *Neisseria gonorrhoeae*, which infects >500,000 people per year in the  
63 US (2). Bacterial ribosome rescue pathways have been proposed as potential antibiotic  
64 targets because they are essential in bacteria and are highly dissimilar from cytoplasmic  
65 mechanisms to disassemble non-stop ribosomes in eukaryotes (3). Bacterial ribosomes

66 frequently stall at the 3' end of mRNAs lacking an in-frame stop codon, due to physical or  
67 nucleolytic damage to the mRNA or premature termination of transcription (4). These  
68 "non-stop" ribosomes must be rescued to maintain protein synthesis capacity and cell  
69 viability (4). All bacterial species that have been studied use *trans*-translation as the  
70 primary ribosome rescue pathway. During *trans*-translation, transfer-messenger RNA  
71 (tmRNA) and the protein SmpB recognize non-stop ribosomes and use tRNA-like and  
72 mRNA-like properties of tmRNA to add a short sequence to the nascent polypeptide and  
73 terminate translation at a stop codon within tmRNA (4). In some bacteria, including *N.*  
74 *gonorrhoeae*, tmRNA and SmpB are essential (5, 6). Other species have an alternative  
75 ribosome rescue factor (ArfA, ArfB, ArfT, or BrfA) that acts as a backup system for  
76 rescuing ribosomes when *trans*-translation activity is not sufficient (7–10). Deletions of  
77 the alternative ribosome rescue factors and tmRNA or SmpB are synthetically lethal,  
78 indicating that at least one mechanism for ribosome rescue is required for bacterial  
79 viability (5).

80 A family of acylaminooxadiazoles identified in a high-throughput screen for  
81 inhibitors of *trans*-translation in *Escherichia coli* was shown to have broad-spectrum  
82 antibiotic activity *in vitro* (3, 11). Experiments in *E. coli* and *Mycobacterium smegmatis*  
83 showed that KKL-2098, a cross-linkable acylaminooxadiazole derivative, bound 23S  
84 rRNA near the peptidyl-transfer center (PTC), suggesting that these molecules inhibit  
85 *trans*-translation by binding the ribosome (11). Based on these data, we sought to  
86 optimize the acylaminooxadiazole activity against *N. gonorrhoeae* and establish the basis  
87 for selective inhibition of *trans*-translation.

88 Evaluation of *in vitro* pharmacokinetic properties of the original hit, KKL-35,

89 revealed that the amide bond is rapidly hydrolyzed in liver microsomes, making it  
90 unsuitable for animal studies (Fig. 1, Table S1). To enable animal studies, >500 analogs  
91 of KKL-35 were designed and evaluated for potency, toxicity, and pharmacokinetic  
92 properties (Fig. 1, Table S1). Compound potency, assessed by minimum inhibitory  
93 concentration (MIC) against *N. gonorrhoeae* and activity (EC<sub>50</sub>) in a *trans*-translation  
94 luciferase reporter assay (3), was responsive to structural changes, consistent with  
95 specific binding of the molecule to the target (Fig. 1, Table S1). Conceptually, the  
96 compound can be divided into 4 distinct zones (Fig. 1A). The central portion (Zones 2 and  
97 3) played a critical role in activity, and the termini (Zones 1 and 4) tolerated changes that  
98 facilitated tuning physical properties and potency. A key finding of these experiments was  
99 that replacement of the Zone 3 amide with a urea dramatically improved metabolic  
100 stability without significantly decreasing potency (Fig. 1, Table S1). MBX-4132, a  
101 uriedooxadiazole, exhibited excellent stability in both murine liver microsomes and murine  
102 serum as well as excellent Caco-2 permeability (Fig. 1B, Table S2). MBX-4132 inhibited  
103 *trans*-translation both in the *E. coli* luciferase reporter assay (Fig. 1B) and in an *in vitro*  
104 reconstituted assay (IC<sub>50</sub> = 60 nM), but did not inhibit translation *in vitro* (Fig. 1D).

105 Like the parent acylaminooxadiazole compounds, MBX-4132 exhibited potent  
106 broad-spectrum antibiotic activity against Gram-positive species and many Gram-  
107 negative species, including *N. gonorrhoeae* (Fig. 1, Tables S3 & S4). The prevalence of  
108 multiple-drug resistant (MDR) strains of *N. gonorrhoeae* has made infections increasingly  
109 difficult to treat (2). MBX-4132 was highly effective against all tested clinical isolates of *N.*  
110 *gonorrhoeae*, including MDR strains (Fig. 1, Table S3), indicating that prevalent  
111 resistance mechanisms are not active against MBX-4132. The frequency of spontaneous

112 mutants resistant to MBX-4132 was  $<1.2 \times 10^{-9}$ , suggesting that emergence of resistance  
113 in the clinic is likely to be slow. Time-kill assays demonstrated that MBX-4132 was  
114 bactericidal to *N. gonorrhoeae* at concentrations  $\geq 4X$  MIC (Fig. 1E).

115 *In vitro* analyses indicate that MBX-4132 is likely to have low toxicity in mammals.  
116 Measurement of competitive binding with 45 mammalian receptors, inhibition of 7 cardiac  
117 ion channels, inhibition of the 5 major liver CYP450 enzymes, and an Ames assay for  
118 genotoxicity revealed minimal off-target activity, with only minor inhibition of two  
119 mammalian receptors observed (Tables S5 & S6). Additionally, high concentrations of  
120 MBX-4132 had no effect on mitochondrial membrane polarity in human hepatocytes  
121 although elevated levels of reactive oxygen species (ROS) were observed at cytotoxic  
122 compound concentrations (Table S7). Likewise, MBX-4132 did not induce differential  
123 toxicity against HepG2 cells in the presence of either Glu or Gal, consistent with normal  
124 mitochondrial metabolism (Table S7). Collectively, these data show that MBX-4132 is an  
125 extremely promising lead candidate suitable for further development.

126 Pharmacokinetic testing of MBX-4132 revealed that the compound was highly  
127 orally bioavailable in mice, exhibiting excellent plasma exposure (area under the curve;  
128 AUC), half-life ( $t_{1/2}$ ) and a low clearance rate (Fig. S1). Moreover, animals exhibited no  
129 obvious adverse effects at a single dose of 100 mg/kg, or repeat dosing at 10 mg/kg (BID,  
130 7 d). Based on these results and the *in vitro* potency against *N. gonorrhoeae*, we  
131 investigated the efficacy of MBX-4132 in a murine genital tract infection model (12–15).  
132 Lower genital tract infection was established with the *N. gonorrhoeae* clinical isolate  
133 H041, which is resistant to at least 7 classes of antibiotics (16), and mice were treated  
134 either with daily intraperitoneal injection of 48 mg/kg gentamicin for 5 days or with a single

135 oral dose of 10 mg/kg MBX-4132 (n = 20–21 mice/group). As previously observed (13),  
136 daily intraperitoneal injection of gentamicin was effective against H041, clearing infection  
137 in 95% of treated mice (Fig. 2A). A single oral dose of MBX-4132 also showed significant  
138 efficacy, with 80% of mice completely cleared of infection by 6 days, and a dramatic  
139 reduction in bacterial load (Fig. 2). These data are the first *in vivo* proof-of-concept that  
140 inhibition of *trans*-translation is a viable antibiotic strategy.

141 To further understand the mechanism of the acylaminooxadiazole antibiotics, we  
142 used cryogenic electron microscopy (cryo-EM) to determine the structure of KKL-2098  
143 cross-linked to a non-stop ribosome (Figs. 3 & S2, Table S8). Non-stop ribosomes were  
144 generated in *E. coli* by over-expression of an mRNA that contains an RNase III cleavage  
145 site before the stop codon and encodes a protein with a histidine tag at the N terminus.  
146 Endogenous RNase III cuts this mRNA *in vivo*, and translation produces non-stop  
147 ribosomes with the histidine tag from the nascent polypeptide extending from the peptide  
148 tunnel. KKL-2098 was added to the culture, UV radiation was used to stimulate cross-  
149 linking between KKL-2098 and the ribosomes, and the non-stop ribosomes were affinity-  
150 purified, vitrified, and visualized by cryo-EM. 474,382 particles were collected and  
151 classified to isolate the 70S ribosomes containing a P-site tRNA, and the structure was  
152 solved to 3.1 Å resolution (Figs. S2, S3, S4). Inspection of the map revealed density  
153 consistent with KKL-2098 near residue C2452 in the PTC (Fig. S4).

154 KKL-2098 is within 2.1 Å of C2452 (Figs. 3C & S5), the base that was previously  
155 shown to crosslink with KKL-2098 in *E. coli* (3). The position of KKL-2098 indicates it has  
156 hydrophobic interactions with U2506 (Figs. 3C & S5). The amide oxygen is adjacent to  
157 the 3' end of the terminal A76 from the P-site tRNA, and N3 of the oxadiazole is adjacent

158 to A2602, positioned to make hydrogen-bonding or dipole interactions that require the  
159 1,3,4 oxadiazole configuration (note that this oxadiazole configuration has a strong dipole  
160 moment (17)). These interactions explain why minor changes in Zones 2 and 3  
161 dramatically reduced potency (Table S1). In this position, KKL-2098 overlaps partially  
162 with the location of the phosphate of A76 (Fig. S6). The binding site of KKL-2098 is likely  
163 to inhibit entry of A-site ligands, including tmRNA-SmpB, into the PTC. Although the  
164 binding site of KKL-2098 has some overlap with the adenosine moiety of puromycin, the  
165 overall binding sites of KKL-2098 and puromycin are distinct, revealing why these drugs  
166 have different mechanisms of action (Fig. S6).

167 Although no major rearrangements in the rRNA core of the PTC were observed,  
168 the N-terminal 7 residues of ribosomal protein L27 move ~180° from the PTC (Fig. 3D).  
169 This position is >25 Å from its position in ribosomes containing a peptidyl-tRNA in the P  
170 site (18–20) (Fig. S7). As is the case for many ribosomal proteins, the first 20 residues of  
171 L27 form a long extension that lacks secondary structure and thus these residues are  
172 frequently not resolved in structures of 70S ribosomes lacking A-site tRNA due to lower  
173 resolution. Cross-linking and biochemical studies showed that the N terminus of L27  
174 extends to the 3' end of the P-site tRNA and stabilizes product formation of the peptidyl  
175 transferase reaction (17)(21–23). Consistent with these data, the N terminus has been  
176 observed to extend parallel to the 3' end of the P-site tRNA in structures containing either  
177 peptidyl P-site tRNAs or aminoacylated tRNAs at the A site (18–20). In the KKL-2098-  
178 bound structure, the N terminus bends 180° at Gly8 and packs against ribosomal protein  
179 L16 and the acceptor stem of the P-site tRNA. These two positions suggest the N  
180 terminus of L27 is mobile and its movement may be required for optimal function such as

181 in *trans*-translation or peptide release by any alternative rescue factors. In addition,  
182 single-particle reconstruction of non-stop ribosomes lacking a P-site tRNA but containing  
183 KKL-2098 also showed the rotated conformation of L27, suggesting that this conformation  
184 is preferred when an acylaminooxadiazole is bound (Fig. S7).

185 To test whether the position of L27 plays a role in acylaminooxadiazole activity, we  
186 examined the effects of *E. coli* mutants that are truncated by 3 or 6 residues from the N  
187 terminus, preventing L27 from reaching the PTC and the location of acylaminooxadiazole  
188 binding. Both mutants were hypersensitive to MBX-4132, but not to other antibiotics that  
189 target the ribosome, indicating that absence of L27 from the PTC increases sensitivity to  
190 MBX-4132 (Fig. 4).

191 The movement of L27 also provides a possible explanation for why MBX-4132  
192 specifically inhibits *trans*-translation and not translation elongation. Extension of L27 into  
193 the PTC in translation elongation complexes would disfavor MBX-4132 binding, but  
194 rotation of L27 in non-stop ribosomes could allow MBX-4132 binding and inhibition of  
195 *trans*-translation. Although further experiments will be required to test this model, it is  
196 clear that the acylaminooxadiazoles exhibit a novel mechanism of antibacterial activity.  
197 Taken together, the specific inhibition of *trans*-translation by acylaminooxadiazoles and  
198 significant *in vivo* efficacy against *N. gonorrhoeae* after a single oral dose, combined with  
199 the new chemical structure, support further development of these compounds as  
200 promising new antibiotics.

201

202 **ACKNOWLEDGEMENTS**

203  
204 We are grateful to Shura Mankin for providing L27 mutants; Tim Murphy and the staff at Neosome  
205 Life Sciences LLC for support in performing and evaluating murine tolerability studies; Charles  
206 River Labs, for performing murine pharmacokinetic studies; Micromyx for performing MIC90  
207 studies; Eurofins Panlabs, RTI International and SRI Biosciences for performing extensive *in vitro*  
208 safety screening studies. Funding and support for this research was provided by NIH grant  
209 R01GM121650 to KCK and by NIAID preclinical contract services, NIH grant R43AI141132 to  
210 ZDA, and R01AI132276 to ZDA.

211

212

213 **REFERENCES**

214

- 215 1. Interagency Coordination Group on Antimicrobial Resistance, "WHO | No Time to Wait:  
216 Securing the future from drug-resistant infections" (World Health Organization, 2019),  
217 (available at <http://www.who.int/antimicrobial-resistance/interagency-coordination-group/final-report/en/>).
- 219 2. U. S. Department of Health and Human Services CDC, "CDC. Antibiotic Resistance Threats  
220 in the United States, 2019." (Atlanta, GA, 2019), p. 148.
- 221 3. N. S. Ramadoss, J. N. Alumasa, L. Cheng, Y. Wang, S. Li, B. S. Chambers, H. Chang, A. K.  
222 Chatterjee, A. Brinker, I. H. Engels, K. C. Keiler, Small molecule inhibitors of trans-  
223 translation have broad-spectrum antibiotic activity. *Proc. Natl. Acad. Sci. U. S. A.* **110**,  
224 10282–10287 (2013).
- 225 4. K. C. Keiler, Mechanisms of ribosome rescue in bacteria. *Nat. Rev. Microbiol.* **13**, 285–297  
226 (2015).
- 227 5. K. C. Keiler, H. A. Feaga, Resolving nonstop translation complexes is a matter of life or  
228 death. *J. Bacteriol.* **196**, 2123–2130 (2014).
- 229 6. C. Huang, M. C. Wolfgang, J. Withey, M. Koomey, D. I. Friedman, Charged tmRNA but not  
230 tmRNA-mediated proteolysis is essential for *Neisseria gonorrhoeae* viability. *EMBO J.* **19**,  
231 1098–1107 (2000).
- 232 7. T. D. P. Goralski, G. S. Kirimanjeswara, K. C. Keiler, A New Mechanism for Ribosome Rescue  
233 Can Recruit RF1 or RF2 to Nonstop Ribosomes. *mBio*. **9**, 2123 (2018).
- 234 8. Y. Chadani, K. Ono, K. Kutsukake, T. Abo, *Escherichia coli* YaeJ protein mediates a novel  
235 ribosome-rescue pathway distinct from SsrA- and ArfA-mediated pathways. *Mol.*  
236 *Microbiol.* **80**, 772–785 (2011).

237 9. H. A. Feaga, P. H. Viollier, K. C. Keiler, Release of nonstop ribosomes is essential. *mBio*. **5**,  
238 e01916 (2014).

239 10. N. Shimokawa-Chiba, C. Müller, K. Fujiwara, B. Beckert, K. Ito, D. N. Wilson, S. Chiba,  
240 Release factor-dependent ribosome rescue by BrfA in the Gram-positive bacterium  
241 *Bacillus subtilis*. *Nat. Commun.* **10**, 5397 (2019).

242 11. J. N. Alumasa, P. S. Manzanillo, N. D. Peterson, T. Lundrigan, A. D. Baughn, J. S. Cox, K. C.  
243 Keiler, Ribosome Rescue Inhibitors Kill Actively Growing and Nonreplicating Persister  
244 *Mycobacterium tuberculosis* Cells. *ACS Infect. Dis.* **3**, 634–644 (2017).

245 12. A. E. Jerse, H. Wu, M. Packiam, R. A. Vonck, A. A. Begum, L. E. Garvin, Estradiol-Treated  
246 Female Mice as Surrogate Hosts for *Neisseria gonorrhoeae* Genital Tract Infections. *Front.*  
247 *Microbiol.* **2**, 107 (2011), doi:10.3389/fmicb.2011.00107.

248 13. M. M. Butler, S. L. Waidyarachchi, K. L. Connolly, A. E. Jerse, W. Chai, R. E. Lee, S. A.  
249 Kohlhoff, D. L. Shinabarger, T. L. Bowlin, Aminomethyl Spectinomycins as Therapeutics for  
250 Drug-Resistant Gonorrhea and Chlamydia Coinfections. *Antimicrob. Agents Chemother.* **62**  
251 (2018), doi:10.1128/AAC.00325-18.

252 14. K. L. Connolly, A. E. Eakin, C. Gomez, B. L. Osborn, M. Unemo, A. E. Jerse, Pharmacokinetic  
253 Data Are Predictive of In Vivo Efficacy for Cefixime and Ceftriaxone against Susceptible and  
254 Resistant *Neisseria gonorrhoeae* Strains in the Gonorrhea Mouse Model. *Antimicrob.*  
255 *Agents Chemother.* **63** (2019), doi:10.1128/AAC.01644-18.

256 15. D. M. Schmitt, K. L. Connolly, A. E. Jerse, M. S. Detrick, J. Horzempa, Antibacterial activity  
257 of resazurin-based compounds against *Neisseria gonorrhoeae* in vitro and in vivo. *Int. J.*  
258 *Antimicrob. Agents.* **48**, 367–372 (2016).

259 16. M. Ohnishi, D. Golparian, K. Shimuta, T. Saika, S. Hoshina, K. Iwasaku, S. Nakayama, J.  
260 Kitawaki, M. Unemo, Is *Neisseria gonorrhoeae* Initiating a Future Era of Untreatable  
261 Gonorrhea?: Detailed Characterization of the First Strain with High-Level Resistance to  
262 Ceftriaxone. *Antimicrob. Agents Chemother.* **55**, 3538–3545 (2011).

263 17. J. Boström, A. Hogner, A. Llinàs, E. Wellner, A. T. Plowright, Oxadiazoles in Medicinal  
264 Chemistry. *J. Med. Chem.* **55**, 1817–1830 (2012).

265 18. Y. S. Polikanov, T. A. Steitz, C. A. Innis, A proton wire to couple aminoacyl-tRNA  
266 accommodation and peptide-bond formation on the ribosome. *Nat. Struct. Mol. Biol.* **21**,  
267 787–793 (2014).

268 19. P. Huter, S. Arenz, L. V. Bock, M. Graf, J. O. Frister, A. Heuer, L. Peil, A. L. Starosta, I.  
269 Wohlgemuth, F. Peske, J. Nováček, O. Berninghausen, H. Grubmüller, T. Tenson, R.  
270 Beckmann, M. V. Rodnina, A. C. Vaiana, D. N. Wilson, Structural Basis for Polyproline-  
271 Mediated Ribosome Stalling and Rescue by the Translation Elongation Factor EF-P. *Mol.*  
272 *Cell.* **68**, 515–527.e6 (2017).

273 20. R. M. Voorhees, A. Weixlbaumer, D. Loakes, A. C. Kelley, V. Ramakrishnan, Insights into  
274 substrate stabilization from snapshots of the peptidyl transferase center of the intact 70S  
275 ribosome. *Nat. Struct. Mol. Biol.* **16**, 528–533 (2009).

276 21. B. A. Maguire, A. D. Beniaminov, H. Ramu, A. S. Mankin, R. A. Zimmermann, A Protein  
277 Component at the Heart of an RNA Machine: The Importance of Protein L27 for the  
278 Function of the Bacterial Ribosome. *Mol. Cell.* **20**, 427–435 (2005).

279 22. I. K. Wower, J. Wower, R. A. Zimmermann, Ribosomal Protein L27 Participates in both 50 S  
280 Subunit Assembly and the Peptidyl Transferase Reaction. *J. Biol. Chem.* **273**, 19847–19852  
281 (1998).

282 23. J. Wower, S. V. Kirillov, I. K. Wower, S. Guven, S. S. Hixson, R. A. Zimmermann, Transit of  
283 tRNA through the *Escherichia coli* Ribosome: Cross-Linking of the 3' End of tRNA to Specific  
284 Nucleotides of the 23 S Ribosomal RNA at the A, P, and E Sites. *J. Biol. Chem.* **275**, 37887–  
285 37894 (2000).

286

287

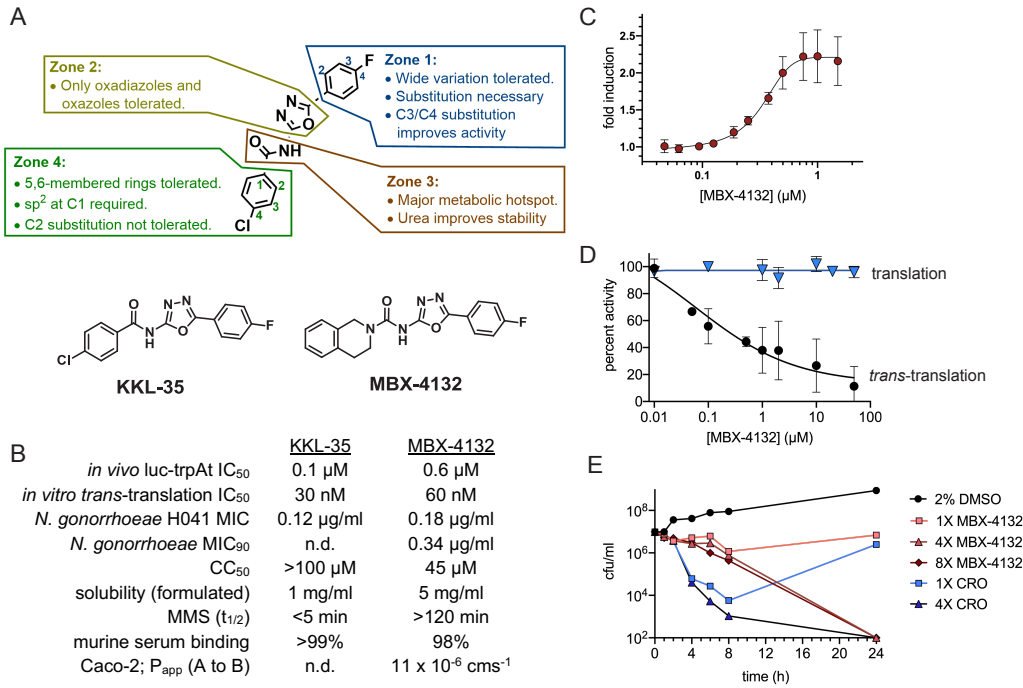
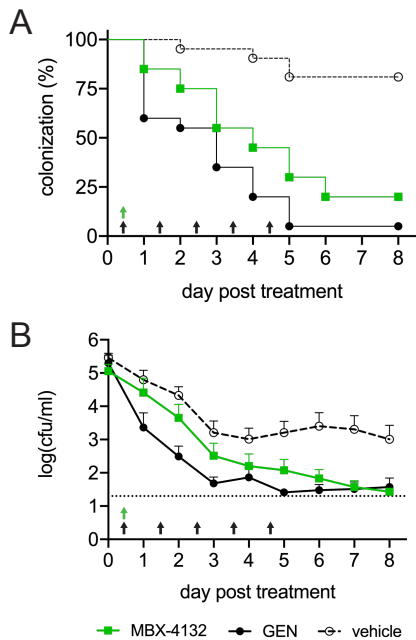


**Figure 1. Optimized acylaminooxadiazoles inhibit *trans*-translation to kill *N. gonorrhoeae*.** (A) Zones used to guide synthetic strategy with characteristics that govern activity are indicated, and the structure of KKL-35 and MBX-4132 are shown. (B) Properties of the initial hit, KKL-35, and optimized inhibitor MBX-4132 (CC<sub>50</sub> – half-maximal cytotoxic concentration against HeLa cells; MMS – murine liver microsome stability). (C) Inhibition of *trans*-translation in *E. coli* cells was monitored using a non-stop luciferase reporter. The average of two biological repeats is shown with error bars indicating standard deviations. (D) Inhibition of *trans*-translation *in vitro* was assayed using an *E. coli* S12 extract to express a truncated, non-stop nano-luciferase gene in the presence of a mutant tmRNA that added the remainder of the nano-luciferase protein. *Trans*-translation activity resulted in luminescence, and addition of MBX-4132 inhibited the reaction (black). As a control, a full-length nano-luciferase gene was used to demonstrate that MBX-4132 does not inhibit translation (blue). The percentage of activity compared to activity in absence of MBX-4132 is shown from the average of at least three repeats with error bars indicating standard deviation. (E) Time-kill assays using *N. gonorrhoeae* show that MBX-4132 is bactericidal at  $\geq 4$ X MIC. Ceftriaxone (CRO) was used as a control. Counts below the detection limit (100 cfu/ml) were plotted at 100 cfu/ml.



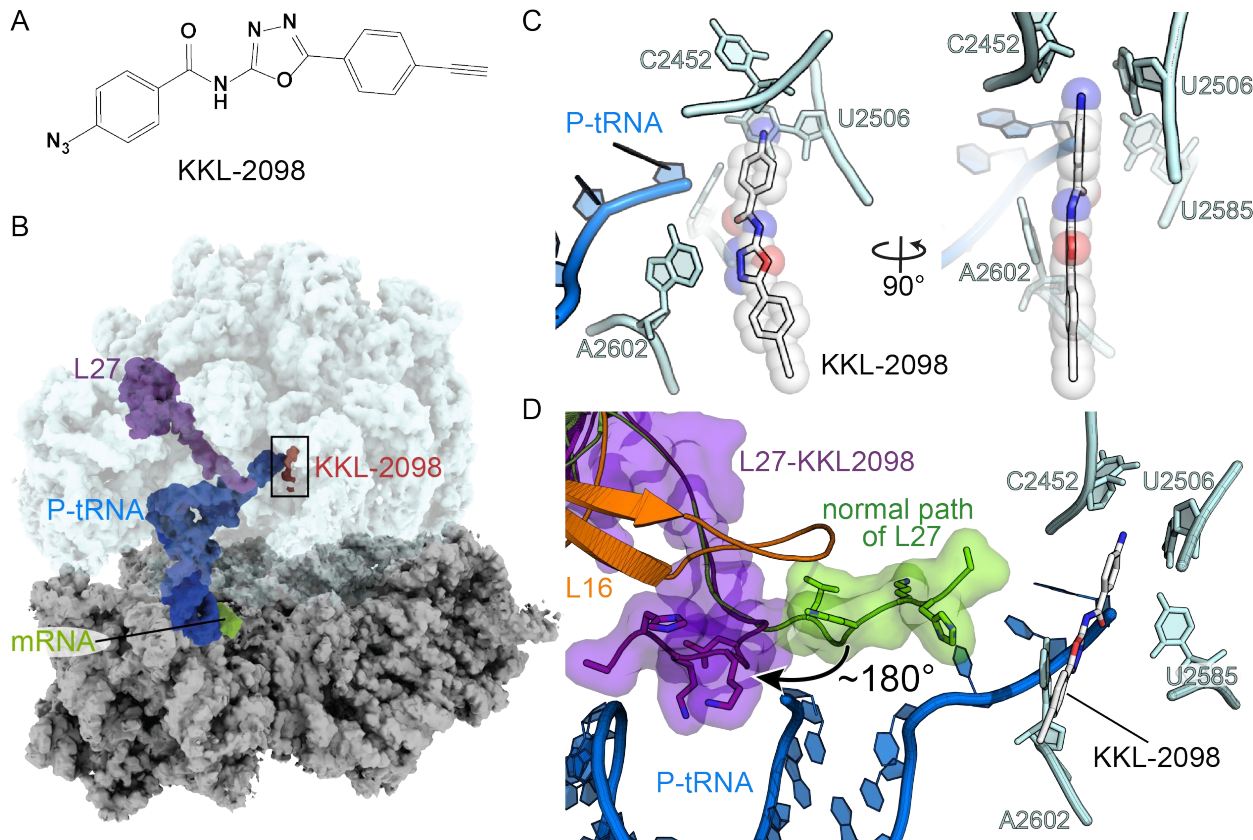
289

290

291

292

**Figure 2. MBX-4132 clears infection by a multiple-antibiotic resistant *N. gonorrhoeae* strain in a murine infection model.** Mice were infected with *N. gonorrhoeae* H041 for two days and treated with a single oral dose of 10 mg/kg MBX-4132 or vehicle on day 0 (green arrow), (n = 20 – 21 mice/group). As a positive control, 48 mg/kg gentamicin (GEN) was administered by intraperitoneal injection beginning on day 0 (5QD, black arrows). (A) The percentage of infected mice over 8 days post-treatment. Mice that were culture-negative for at least 3 consecutive days were considered to have cleared infection. MBX-4132 and GEN significantly reduced the percent of infected mice compared to vehicle ( $p < 0.0001$ ). (B) Average bacterial burden (cfu/ml) recovered daily following treatment on day 0. MBX-4132 and GEN significantly reduced the bacterial burden compared to vehicle ( $p < 0.0001$ ). Limit of detection (20 cfu/ml) is denoted by the horizontal dashed line.



293  
294  
**Figure 3. KKL-2098 binds near the peptidyl transferase center.** (A) The chemical  
295 structure of KKL-2098. (B) The cryo-EM structure of the *E. coli* 70S non-stop ribosome  
296 with P-site tRNA, mRNA, ribosomal protein L27 and KKL-2098 indicated. (C) KKL-2098  
297 is positioned close to the peptidyl transferase center adjacent to 23S rRNA A2602,  
298 C2452, U2506 and U2585 and the CCA end of the P-site tRNA. (D) The N terminus of  
299 L27 (purple) moves 180° to pack against ribosomal protein L16 and the acceptor arm of  
300 the P-site tRNA. The normal position of L27 in translating ribosomes is shown in green  
301 (PDB ID 6ENU).  
302  
303  
304  
305  
306  
307  
308  
309  
310

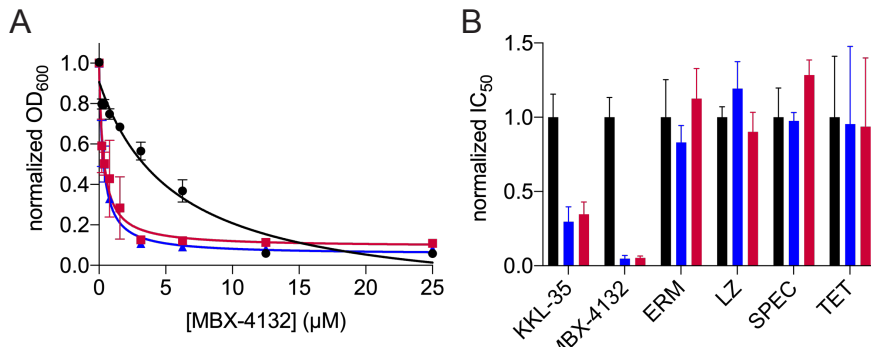


**Figure 4. Truncation of L27 causes hypersensitivity to acylaminooxadiazoles** (A) Growth of *E. coli*  $\Delta$ to/C expressing full-length L27 (black) or variants missing residues 2-5 (-3, blue) or 2-8 (-6, red) was monitored in broth microdilution experiments and the IC<sub>50</sub> for MBX-4132 was determined. Two technical replicates were performed for each biological replicate and the average of three biological replicates is shown with error bars indicating standard deviations. (B) Normalized mean IC<sub>50</sub> values from at least 3 biological replicates of experiments as in (A) show that truncation of L27 increases sensitivity to KKL-35 and MBX-4132 but has no effect on erythromycin (ERM), linezolid (LZ), spectinomycin (SPEC) or tetracycline (TET). Error bars indicate standard deviations.